Anal. Chem. **2008,** *80,* 6554–6559

Molecular Architectures for Electrocatalytic Amplification of Oligonucleotide Hybridization

Mònica Mir,[†] Marta Álvarez,[†] Omar Azzaroni,[*,†,‡] Louis Tiefenauer,[§] and Wolfgang Knoll[†]

Max-Planck-Institut für Polymerforschung, Ackermannweg 10 (55128) Mainz, Germany, INIFTA-UNLP-CONICET, CC 16 Suc. 4 (1900) La Plata, Argentina, and Life Sciences Department, Paul Scherrer Institut, CH-5232 Villigen PSI, Switzerland

In this work, we describe a new platform suitable for electrocatalytic amplification of oligonucleotide hybridization based on the use of supramolecular bioconjugates incorporating ferrocene-labeled streptavidin. Our goals were aimed at designing a biosensing platform which could support highly reproducible and stable electrocatalytic amplification with maximum efficiency. The use of nonlabeled streptavidin as an underlying layer promotes a major improvement on the characteristics of the amplified electrochemical signal. In addition, the electrocatalytic current can be easily amplified by tuning the concentration of electron donor species in solution. Because of the fact that the redox labels are bioconjugated to the DNA strands, increasing the ionic strength does not lead to the loss of redox labels. More importantly, increasing the concentration of donors only involves the magnification of the signal without implying the permeation of donors (thus reducing the efficient electrocatalysis). This approach represents a major improvement on the use of electrocatalytically amplified DNA-sensing platforms, thus overcoming any possible limitation in connection with the reproducibility and reliability of this well-established method.

The development of novel and sensitive methods for the detection of molecular recognition events, like DNA hybridization, became a most relevant topic within the bioanalytical research community.[1,2] Searching for new selective, simple, and reproducible strategies for recognizing DNA hybridization is in close connection with highly demanding research efforts directed to gene analysis, disease control, detection of genetic disorders, or even forensic applications. In order to achieve this goal, different approaches with varying readout systems were discussed in the literature during the past decade. These included the use of acoustic methods,[3] surface plasmon spectroscopy,[4] fluorescence,[5] or luminescence detection.[6] Recently, nanomaterials have been used as read out systems of biorecognition events by exploiting their plasmonic properties in solution[7] or at surfaces.[8] In many cases, interesting approaches were not able to reach any significant technological impact because of the lack of the required combination of reproducibility, accuracy, simplicity, and equally important, low-cost implementation.

Regarding this latter issue, electrochemistry has received increasing attention due to the fact that electrochemical reactions give an electronic signal directly, with no need for expensive signal transduction equipments.[9–14] One important example concerns electrochemical DNA sensors which typically involve the assembly of single-stranded nucleic acid probes (ss-DNA) on the electrode surface followed by hybridization with the complementary target strands (ds-DNA). The electrochemical readout is based on using redox reactions or labels which trigger an electrochemical signal upon the hybridization of the cDNA strand.[15] This can be easily achieved by intercalating redox species in the double-stranded DNA or by labeling the complementary target with an electroactive species.[16] The procedure to introduce the labels is highly dependent on the complexity of the interfacial architecture. For example, in the case of the detection of viral DNA including 7229 bases, interacting redox labeled nucleotides with the double-stranded assembly was demonstrated to be the most convenient strategy.[17] However, with dependence on the density of capture probes, the electrochemical signal can be very low, thus sensitively affecting the applicability of the method.[15]

* To whom correspondence should be addressed. E-mail: azzaroni@mpip-mainz.mpg.de or azzaroni@inifta.unlp.edu.ar.

[†] Max-Planck-Institut für Polymerforschung.

[‡] INIFTA-UNLP-CONICET.

[§] Paul Scherrer Institut.

(1) Pividori, M. I.; Merkoci, A.; Alegret, S. *Biosens. Bioelectron.* **2003**, *19*, 473.
(2) Katz, E.; Willner, I.; Wang, J. *Electroanalysis* **2004**, *16*, 19–44.
(3) Wittung-Stafshede, P.; Rodahl, M.; Kasemo, B.; Nielsen, P.; Norden, B. *Colloids Surf., A* **2000**, *174*, 269–273.
(4) Tawa, K.; Yao, D. F.; Knoll, W. *Biosens. Bioelectron.* **2005**, *21*, 322–329.
(5) Chu, L. Q.; Förch, R.; Knoll, W. *Angew. Chem., Int. Ed.* **2007**, *46*, 4944–4947.
(6) Nordell, P.; Westerlund, F.; Wilhelmsson, L. M.; Nordén, B.; Lincoln, P. *Angew. Chem., Int. Ed.* **2007**, *46*, 2203–2206.
(7) Elghanian, R.; Storhoff, J. J.; Mucic, R. C.; Letsinger, R. L.; Mirkin, C. A. *Science* **1997**, *277*, 1078–1081.
(8) Hutter, E.; Pileni, M. P. *J. Phys. Chem. B* **2003**, *107*, 6497–6499.
(9) Willner, I.; Katz E. In *Bioelectronics: From Theory to Applications*; Willner, I. , Katz, E. , Eds.; Wiley-VCH: Weinheim, Germany, 2005; Chapter 1, 1.
(10) *Molecular Bioelectronics*; Nicolini, C. A. , Ed.; World Scientific: Singapore,1996; Chapter 5, 181.
(11) Patolsky, F.; Lichtenstein, A.; Willner, I. *Nat. Biotechnol.* **2001**, *19*, 253.
(12) Odenthal, K. J.; Gooding, J. J. *Analyst* **2007**, *132*, 603–610.
(13) Gooding, J. J.; King, C. C. *J. Mater. Chem.* **2005**, *15*, 4876–4880.
(14) Wang, J. *Anal. Chim. Acta* **2002**, *469*, 63–71.
(15) Grummond, T. G.; Hill, M. G.; Barton, J. K. *Nat. Biotechnol.* **2003**, *21*, 1192.
(16) Liu, J.; Tian, S.; Tiefenauer, L.; Nielsen, P. E.; Knoll, W. *Anal. Chem.* **2005**, *77*, 2756.
(17) Patolsky, F.; Weizmann, Y.; Willner, I. *J. Am. Chem. Soc.* **2002**, *124*, 770–772.

10.1021/ac800560t CCC: $40.75
Published on Web 07/25/2008

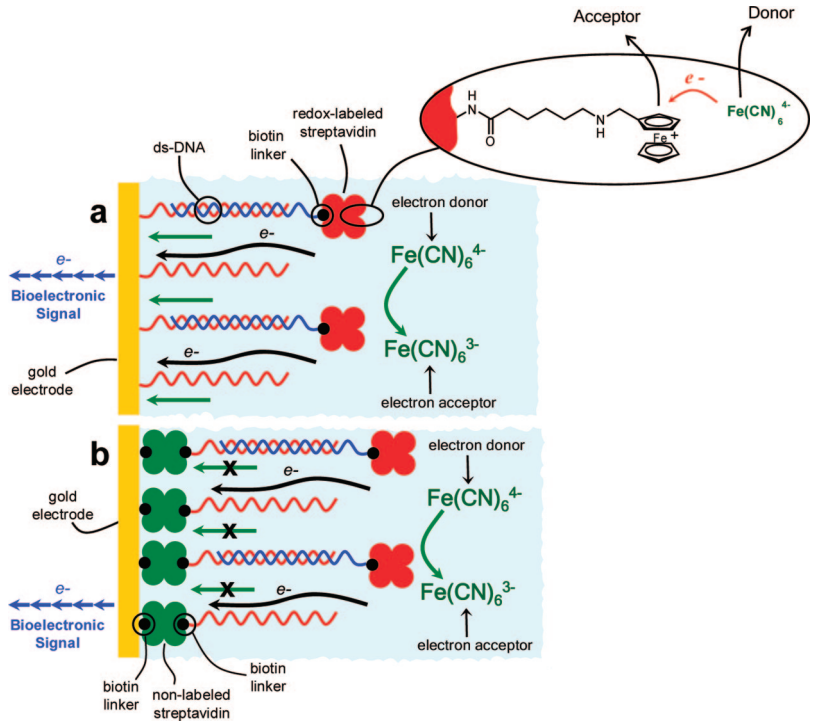

Figure 1. Simplified cartoon describing the different interfacial architectures described in this work: (a) redox-labeled DNA brushes and (b) redox-labeled DNA strands bioconjugated on a SAv platform. The dimensions of the different building blocks are not in scale. The straight green arrows indicate the transport of donor species to the Au interface.

One important breakthrough in the field overcoming this limitation was the use of electrocatalysis to amplify the electrochemical readout. Seminal works of Barton and co-workers demonstrated the use of electrocatalysis as a simple and powerful means to amplify the signal of the redox centers confined to the ds-DNA.[18] Since then, the approach has been successfully implemented for ultrasensitive DNA detection,[19–21] including monitoring pathogenic DNA sequences.[22] However, recent studies revealed a major drawback in the method. It has been demonstrated that the electrocatalytic efficiency, i.e., the amplified signal transduction, could be seriously affected by the characteristics of the biosensor platform. Zhang et al. demonstrated that the efficiency of the electrocatalytic amplification occurring at the capture probe-modified Au electrode was highly dependent on the density and characteristics of the DNA monolayer.[23]

In this work we devoted particular attention to the molecular design of a platform which could support stable electrocatalytic amplification of oligonucleotide hybridization with maximum efficiency, thus overcoming any possible limitation concerning the reproducibility and reliability of this well-established method. To reach this goal we employed a novel approach based on supramolecular bioconjugates obtaining a quantitative improvement on the performance and reproducibility of the method, when compared with the typical platforms for detecting the hybridization of oligonucleotides.

EXPERIMENTAL SECTION

Materials. The oligonucleotide sequences, 19-mer thiol labeled capture probe (SH-C6-5′-TTTTGTACATCACAACTA-3′), 19-mer biotinylated capture probe (biotin-5′-TTTTGTACATCACAACTA-3′) and the biotinylated target (biotin-5′-TAGTTGTGATGTACA-3′) used in this work were purchased from MWG Biotech AG (Germany). Control experiments were performed using the noncomplementary oligonucleotide: (biotin-5′-ATCAGGGTGGGG-GATGGC-3′). All stock oligonucleotide solutions (100 μM) were prepared with autoclaved Milli-Q water and stored at −20 °C. Streptavidin (SAv), 11-mercaptoundecanol, 2-mercaptoethanol, and phosphate buffered saline (PBS) were purchased from Sigma. Biotin-terminated thiol was obtained from Roche Diagnostics. Ferrocene-labeled SAv (Fc-SAv) was synthesized following procedures reported in the literature.[16] Each SAv was labeled with 14 ferrocene units except for the experiments described in Figures 3 and 6, where a conjugate with 9 ferrocene units was used. Electrochemical measurements were carried out with an Autolab potentiostat. The electrochemical cell was a three-electrode system, equipped with a Ag/AgCl reference electrode and a graphite counter electrode.

Preparation of Au/dsDNA/Fc-SAv Platforms. Gold electrodes were incubated in a 1 μM thiolated capture probe solution (using 1 M KH_2PO_4 as a solvent) for 2 h. The assembly was followed by backfilling with 1 mM 2-mercaptoethanol (in water) during 1 h. Hybridization was carried out by incubating the probe-modified gold electrodes in 1 μM biotinylated oligonucleotide target solutions (in 0.1 M PBS buffer) during 1 h at room temperature. Afterward, the biotinylated targets were bioconju-

(18) Boon, E. M.; Ceres, D. M.; Drummond, T. G.; Hill, M. G.; Barton, J. K. *Nat. Biotechnol.* **2000**, *18*, 1096.
(19) Lapierre-Devlin, M. A.; Asher, C. L.; Taft, B. J.; Gasparac, R.; Roberts, M. A.; Kelley, S. O. *Nano Lett.* **2005**, *5*, 1051–1055.
(20) Gasparac, R.; Taft, B. J.; Lapierre-Devlin, M. A.; Lazareck, A. D.; Xu, J. M.; Kelley, S. O. *J. Am. Chem. Soc.* **2004**, *126*, 12270.
(21) Ostatná, V.; Dolinnaya, N.; Andreev, S.; Oretskaya, T.; Wang, J.; Hianik, T. *Bioelectrochemistry* **2005**, *67*, 205.
(22) Lapierre, M. E.; O'Keefe, M.; Taft, B. J.; Kelley, S. O. *Anal. Chem.* **2003**, *75*, 6327.
(23) Zhang, J.; Wang, L.; Pan, D.; Song, S.; Fan, C. *Chem. Commun.* **2007**, 1154.

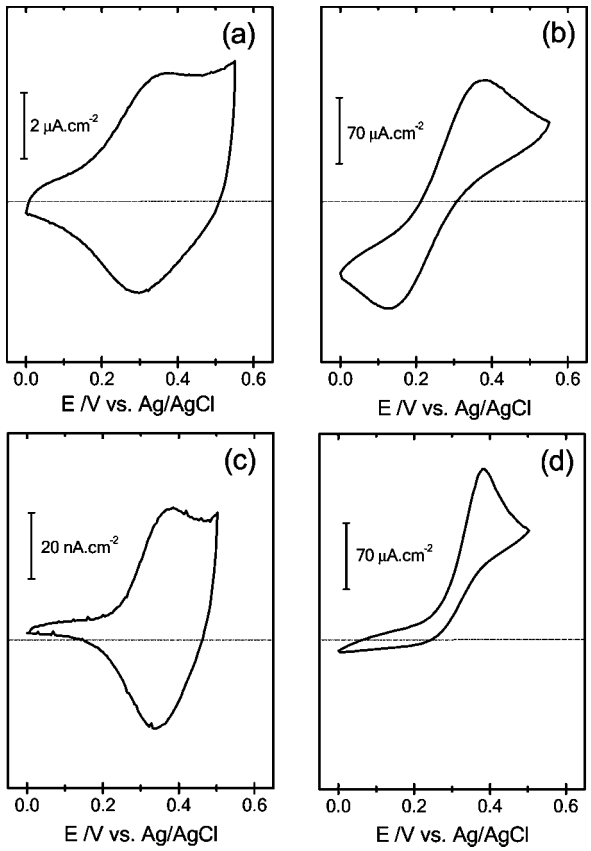

Figure 2. Cyclic voltammograms corresponding to the Au/dsDNA/Fc-SAv platform in (a) 0.1 M PBS buffer and (b) 3 mM $Fe(CN)_6^{4-}$ in PBS; and the Au/SAv/dsDNA/Fc-SAv platform in (c) 0.1 M PBS buffer and (d) 3 mM $Fe(CN)_6^{4-}$ in 0.1 M PBS.

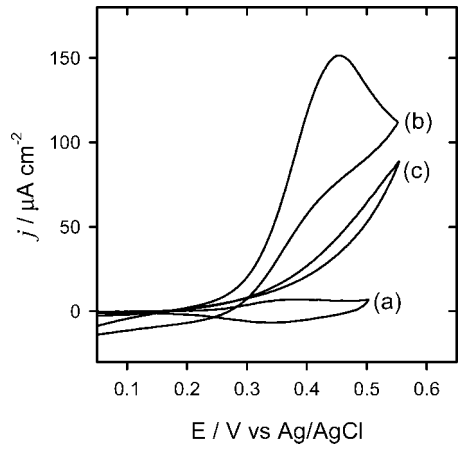

Figure 3. Cyclic voltammograms corresponding to the Au/SAv/ds-DNA/Fc-SAv platform in (a) 0.1 M PBS buffer and (b) 5 mM $Fe(CN)_6^{4-}$ + 0.1 M PBS. (c) Idem to part b for the case of a biotinylated noncomplementary target.

gated with the redox-labeled SAv by placing the biotin-terminated oligonucleotide-modified gold electrodes in contact with 200 nM Fc-SAv solutions (in PBS) during 1 h.

Preparation of Au/SAv/dsDNA/Fc-SAv Platforms. Gold electrodes were immersed during 12 h in a solution containing 0.05 mM biotin-terminated thiol + 0.45 mM 11-mercaptoundecanol (in ethanol). Then, nonlabeled SAv was bioconjugated by immersing the biotinylated gold electrodes in 1 μM SAv solution (in 0.1 M PBS) during 1 h at room temperature. The following step involved the bioconjugation of the biotinylated capture probe on the SAv-terminated gold electrode: immersion in 1 μM biotinylated

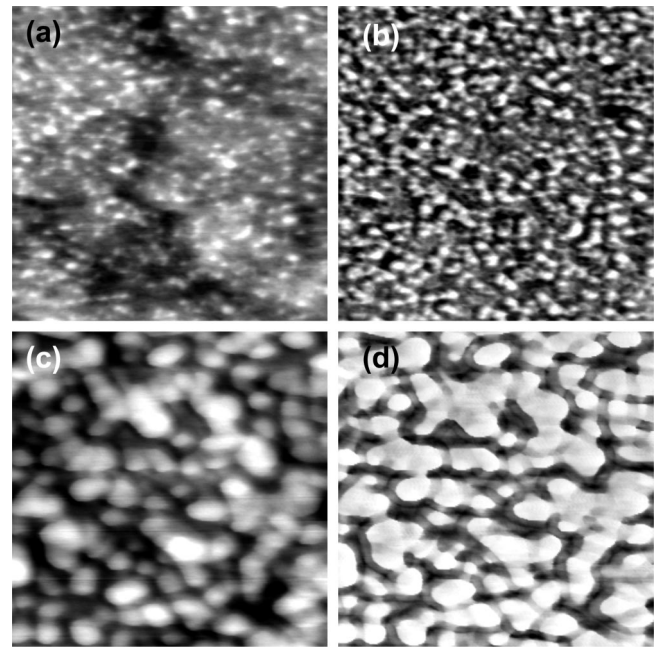

Figure 4. Atomic force microscopy images (500 × 500 nm^2) corresponding to (a) topographic and (b) phase imaging of the Au/ds-DNA/Fc-SAv interfacial architecture; (c) topographic and (d) phase imaging of the Au/SAv/ds-DNA/Fc-SAv platform.

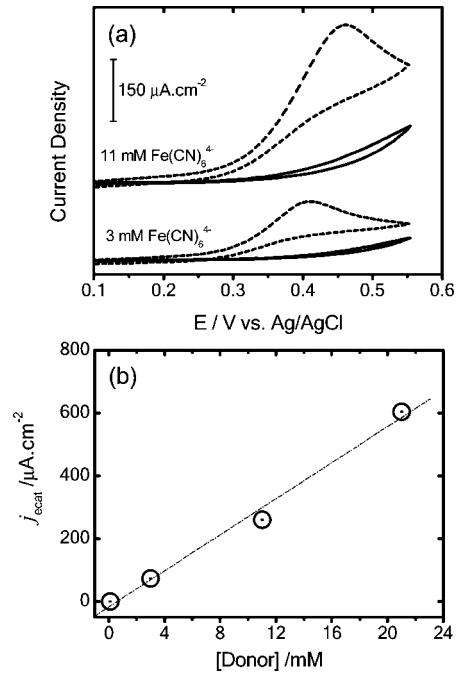

Figure 5. (a) Cyclic voltammograms of the electrocatalytic amplification in different concentrations of $Fe(CN)_6^{4-}$ corresponding to the Au/SAv/ds-DNA platform prior to (solid line) and after (dashed line) bioconjugating the Fc-SAv. Scan rate: 100 mV/s. The voltammograms for the two different concentrations are shifted in the *y*-axis for the sake of clarity. (b) Representation of the electrocatalytic current (j_{ecat}) as a function of the $Fe(CN)_6^{4-}$ (donor) concentration in solution. Electrode: Au/SAv/ds-DNA/Fc-SAv. The error bars are within the size of the symbol.

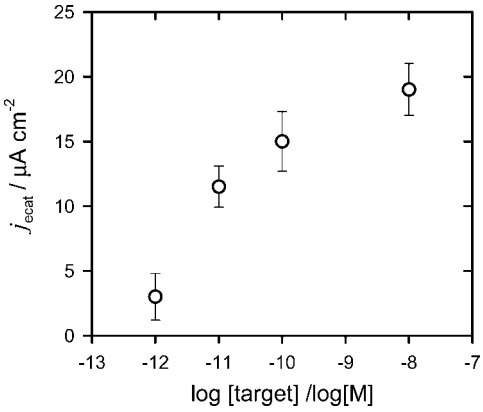

Figure 6. Electrocatalytic current as a function of the target concentration. Redox centers were introduced by labeling the biotinylated DNA-targets with Fc-SAv after hybridization. The electrolyte was 0.1 M PBS buffer containing 1 mM $Fe(CN)_6^{4-}$.

oligonucleotide probe solution (in 0.1 M PBS) during 1 h at room temperature. Once prepared, the oligonucleotide probe layer on the gold electrode, hybridization with target oligonucleotide, and redox labeling proceeded as described above. The same procedure was carried out during control experiments with biotinylated noncomplementary targets.

RESULTS AND DISCUSSION

As stated above, the main drawback about the electrocatalytic amplification concerns its efficiency, i.e., the turning "on" of the electrocatalysis. The principle behind the generation of the amplified electrochemical signal is fairly simple.[24] For example, electron donors (or reducing species) in the solution, which are in contact with electron acceptors (or oxidizing species) in the ds-DNA, are oxidized. Then, if the reverse reaction (where electron acceptors in solution interact with reduced redox labels in the target DNA) is thermodynamically restricted[24] or the electron transport of acceptor to the Au electrode is hindered,[25] no charge transfer will be feasible. The amplification relies on the electrochemical signal originating from the electron transfer between the donor/acceptor in solution and the Au electrode mediated by the redox centers on the ds-DNA. Permeation of acceptors in solution to the Au surface would lead to drastic variations in the electrochemical signal and the current background, thus affecting significantly the reproducibility of the technique.[23]

A most widespread and powerful platform for detecting DNA hybridization consists on the use of DNA brushes.[26–31] It involves the assembly of a monolayer of thiol-terminated capture probes (Figure 1a) followed by backfilling with a hydroxyl-terminated alkanethiol. The backfilling promotes the reorientation of the DNA chains enabling an optimized conformation for a rapid hybridization.[32] We proceeded to the assembly of the thiolated probe (including the backfilling with mercaptoethanol) followed by the hybridization with a biotin-terminated target.

Thereafter, the double-stranded DNA brush was marked by bioconjugating the biotin terminal group with ferrocene-labeled streptavidin.[33–36] Figure 2a shows the cyclic voltammogram corresponding to the Fc-SAv bioconjugated on the biotin-modified double-stranded DNA. The charge associated with the electrochemical signal is $5.4 \pm 0.2\ \mu C/cm^2$, which is equivalent to the presence of $\sim 3.3 \times 10^{13}$ redox centers "wired" to the Au electrode.

To electrocatalytically amplify the readout signal, ferrocyanide species were chosen as electron donors. Cyclic voltammogram in the presence of $Fe(CN)_6^{4-}$ evidence a significant increase in the electrochemical response (Figure 2b). However, the characteristics of this signal do not refer to efficient redox mediation. The appearance of a significant anodic peak indicates the oxidation of $Fe(CN)_6^{4-}$ mediated by the ferrocene label at the bioconjugated ds-DNA. However, one can also observe a cathodic signal originated from the reduction of the electrogenerated $Fe(CN)_6^{3-}$ indicating that the platform is highly permeable to the electroactive species in solution. This observation is in complete agreement with recent results reported by Zhang et al. using thiolated DNA brushes backfilled with mercaptohexanol.[23] Moreover, these results are strongly supported by recent studies reported by Ceres et al. concerning the permeation studies of DNA-modified electrodes.[37] These authors demonstrated that the permselectivity of DNA films was highly dependent on the packing, ionic strength, and nature of the ionic species. All this experimental evidence is a clear indication that the electrocatalytic amplification technique can be deficient when dealing with DNA brushes as a sensing platform. In order to overcome this serious limitation we exploited the versatility of the supramolecular conjugate assembly to introduce modifications on the platform at the molecular level. By exploitation of the biotin−streptavidin biorecognition properties it is easy to create a new electrochemical interface consisting of different building blocks. Initially, we assembled a biotinylated self-assembled monolayer on the Au electrode followed by conjugation of nonlabeled SAv (Figure 1b). It has been demonstrated that this is an excellent platform for immobilizing oligonucleotide probe strands with highly reproducible surface coverage without hindering the hybridization process.[38,39]

Then, biotin-terminated probes were conjugated to the SAv layer. Once the probe molecules were assembled on the SAv-

(24) Alleman, K. S.; Weber, K.; Creager, S. E. *J. Phys. Chem.* **1996**, *100*, 17050.
(25) Savéant,J.-M. *Elements of Molecular and Biomolecular Electrochemistry: An Electrochemical Approach to Electron Transfer Chemistry*; Wiley-Interscience: New York, 2006; Chapter 2, Vol. 78.
(26) Steel, A. B.; Herne, T. M.; Tarlov, M. J. *Anal. Chem.* **1998**, *70*, 4670.
(27) Herne, T. M.; Tarlov, M. J. *J. Am. Chem. Soc.* **1997**, *119*, 8916.
(28) Petrovykh, D. Y.; Kimura-Suda, H.; Whitman, L. J.; Tarlov, M. J. *J. Am. Chem. Soc.* **2003**, *125*, 5219.
(29) Levicky, R.; Horgan, A. *Trends Biotechnol.* **2005**, *23*, 143–149.
(30) Opdahl, A.; Petrovykh, D. Y.; Kimura-Suda, H.; Tarlov, M. J.; Whitman, L. J. *Proc. Natl. Acad. Sci. U.S.A.* **2007**, *104*, 9–14.
(31) Kimura-Suda, H.; Petrovykh, D. Y.; Tarlov, M. J.; Whitman, L. J. *J. Am. Chem. Soc.* **2003**, *125*, 9014–9015.
(32) Arinaga, K.; Rant, U.; Tornow, M.; Fujita, S.; Abstreiter, G.; Yokoyama, N. *Langmuir* **2006**, *22*, 5560–5562.
(33) Padeste, C.; Steiger, B.; Grubelnik, A.; Tiefenauer, L. *Biosens. Bioelectron.* **2004**, *20*, 545.
(34) Steiger, B.; Padeste, C.; Grubelnik, A.; Tiefenauer, L. *Electrochim. Acta* **2003**, *48*, 761.
(35) Padeste, C.; Steiger, B.; Grubelnik, A.; Tiefenauer, L. *Biosens. Bioelectron.* **2003**, *19*, 239.
(36) Padeste, C.; Grubelnik, A.; Tiefenauer, L. *Biosens. Bioelectron.* **2000**, *15*, 431.
(37) Ceres, D. M.; Udit, A. K.; Hill, H. D.; Hill, M. G.; Barton, J. K. *J. Phys. Chem. B* **2007**, *111*, 663.
(38) Knoll, W.; Liley, M.; Piscevic, D.; Spinke, J.; Tarlov, M. J. *Adv. Biophys.* **1997**, *34*, 231.
(39) Liebermann, T.; Knoll, W.; Sluka, P.; Herrmann, R. *Colloids Surf., A* **2000**, *169*, 337–350.

modified surface, the hybridization process with the biotinylated complementary target was carried out. The typical coverages determined by SPR at high oligonucleotide concentrations (1 μM) are SAv, 4×10^{-12} mol/cm^2; ss-DNA, 3.5×10^{-12} mol/cm^2; and ds-DNA, 3×10^{-12} mol/cm^2. These results indicate that in our case the hybridization efficiency is ~85%. This estimation is in good agreement with recent results from Su et al.[40] and Peterson et al.[41] reporting the hybridization efficiency on different platforms with values of 56−79% and 40−80%, respectively.

Thereafter, the hybridization was followed by the conjugation with Fc-SAv. Interestingly, cyclic voltammetry of this supramolecularly conjugated "sandwich" reveals that the electron transfer between the redox labels and the gold electrode is not totally hindered by the presence of a nonlabeled SAv layer in the underlying region of the biosensing platform (Figure 2c). It is worthwhile noticing that in this case, the charge associated with the electrochemical signal is 450 ± 20 nC/cm^2, corresponding to ~2.8×10^{12} active redox centers per cm^2, which is about 10 times less compared to the platform without a SAv-layer on the electrode. This implies that the architecture of the assembly sensitively affects the number of electrochemically active redox centers. The present interfacial architecture relies on three building blocks: the capture probe, the target oligonucleotide, and the Fc-SAv, acting as a reporter. Even if it is demonstrated that Fc-SAv is conjugated to the biotinylated ds-DNA, this does not imply that each ds-DNA is coordinated to an Fc-SAv. The steric hindrance between different Fc-SAv molecules conjugating the biotinylated targets would probably impact the maximum density of redox labels that can be achieved.

Once the electroactivity of the redox-labeled bioconjugated platform was confirmed, the electrocatalytical amplification was demonstrated. Figure 2d displays the cyclic voltammetry of the redox-labeled "supramolecular sandwich" in the presence of $Fe(CN)_6^{4-}$. A well-defined anodic peak can be observed, while the cathodic peak is absent. The differences with respect to the redox-labeled DNA brush are notable and quantitative. This can be attributed to the fact that the underlying protein layer blocks the transport of electroactive species in solution to the Au interface.[24] This is a clear evidence of an optimized interfacial architecture where the efficiency of the amplified electrocatalytic current is ~100% without major contributions from the current background. This means that the detected signal originated exclusively from the mediation of the redox-labeled hybridized targets, thus enabling the facile amplification of the read-out signal using the electrocatalytic process occurring at the interface.

This is further illustrated in Figure 3 showing the magnitude of the electrochemical read out in the absence and in the presence of $Fe(CN)_6^{4-}$ in solution (after proceeding to the hybridization of the complementary target and the labeling with Fc-SAv). The figure also displays the characteristics of the electrochemical read out with a biotinylated noncomplementary target. We observed no electrocatalytic signal thus confirming that hybridization does not occur if noncomplementary oligonucletide targets are used. Thus, the interfacial architecture consisting of SAv and ds-DNA leads to a good sensing specificity.

Both platforms, DNA brushes and SAv/DNA, differ notably in topology upon bioconjugation of the redox mediator (Fc-SAv). Atomic force microscopy (AFM) images after the conjugation of Fc-SAv on the biotin-terminated ds-DNA brush indicates small aggregates evenly distributed (Figure 4a,b). These aggregates could be attributed to the presence of the protein on top of the DNA strands. In contrast, analogous imaging of SAv-dsDNA pretreated electrodes revealed an architecture of nodular aggregates (Figure 4c,d). Topographic and phase imaging clearly show the 3D character of the interfacial architecture generated by assembling the building blocks onto the SAv platform. These images visualize the striking electrochemical differences found for the both interfacial architectures.

In a next step, the versatility of the redox-labeled bioconjugate for the amplification of electrocatalytic signals has to be shown considering the relatively low number of redox centers actually connected to the readout system. In spite of the improved electrocatalytic efficiency, the nature of the interfacial architecture decreases by about 1 order of magnitude the population of "wired" redox centers, thus impacting the magnitude of the electrocatalytic signal. A further challenge remains in increasing the electrocatalytic signal without changing the bioconjugate architecture. Different research groups[42–45] have described the current generated at an electrode containing surface-confined redox sites undergoing bimolecular electron transfer reactions with electron donor/acceptors in solution, i.e., electrocatalytic amplification. In that case the overall current density (j) is[45]

$$j = Fk_{\text{cross}}\Gamma_o c_D \qquad (1)$$

where F is the Faraday constant, k_{cross} is the rate constant for the bimolecular reaction, Γ_o is the surface coverage of redox active sites, and c_D is the concentration of donor (or acceptor) species in solution. From eq 1 it is clear that the electrocatalytic current is proportional to the concentration of donor species in solution, $Fe(CN)_6^{4-}$.

This could be demonstrated using 11 mM $Fe(CN)_6^{4-}$ instead of 3 mM resulting in a pronounced increase of the electrocatalytic current (Figure 5a) without any evidence of permeation of the donor species to the Au electrode (cathodic signal due to electrochemically generated $Fe(CN)_6^{3-}$). As previously discussed, the electrocatalytic signal originates exclusively from the mediation of the redox-labeled hybridized targets. Figure 5a displays the voltammograms corresponding to the Au/SAv/ds-DNA platforms in the presence of $Fe(CN)_6^{4-}$ species prior to and after the bioconjugation of Fc-SAv. It is clearly observed that, for both $Fe(CN)_6^{4-}$ concentrations, the electrocatalysis is "turned on" only in the presence of the redox labels. This means that the sensitivity of the electrocatalytic readout can be easily tuned by setting the donor concentration in solution. Varying the $Fe(CN)_6^{4-}$ concentration from 120 μM to 21 mM leads to a linear increase of the electrocatalytic current (Figure 5b).

Moreover, eq 1 also indicates that the electrocatalytic current is dependent on the surface density of redox centers on the

(40) Su, X.; Wu, Y.-J.; Knoll, W. *Biosens. Bioelectron.* **2005**, *21*, 719–726.
(41) Peterson, A. W.; Wolf, L. K.; Georgiadis, R. N. *J. Am. Chem. Soc.* **2002**, *124*, 14601–14607.
(42) Xie, Y.; Anson, F. C. *J. Electroanal. Chem.* **1995**, *384*, 145–153.
(43) Amarasinghe, S.; Chen, T.; Moberg, P.; Paul, H. J.; Tinoco, F.; Zook, L. A.; Leddy, J. *Anal. Chim. Acta* **1995**, *307*, 227–244.
(44) Andrieux, C. P.; Dumas-Bouchiat, J. M.; Savéant, J. M. *J. Electroanal. Chem.* **1982**, *131*, 1–35.
(45) Creager, S. E.; Radford, P. T. *J. Electroanal. Chem.* **2001**, *500*, 21–29.

electrode. In our case, the presence of the redox centers (which promote the electrocatalysis) on the platform is due to the labeling of the biotinylated oligonucleotide target with Fc-SAv. In other words, the density of electroactive redox labels is exclusively and solely related to the biotinylated targets hybridized on the electrode surface.

This fact would indicate proportionality between the target concentration and the electrocatalytic readout. In order to verify this assumption and check the sensitivity limits of the platform, we proceeded to study the electrocatalytic amplification in the presence of target concentrations below 10^{-8} M.

Figure 6 shows the dependence of the amplified electrocatalytic current as a function of the target concentration. As expected, it can be clearly recognized that (a) there is a good correlation between j_{ecat} and the target concentration and (b) the supramolecularly bioconjugated platform is extremely sensitive and target concentrations in the 10^{-8}–10^{-12} range are detectable. This sensitivity is comparable to that of current electrochemical methods for DNA detection.[46] Control experiments indicated that working with target concentrations below 10^{-12} M will be difficult because of the very low (but electrocatalytically detectable) level of nonspecific adsorption of Fc-SAv.

CONCLUSIONS

In summary, in this work we have described a new approach for a biosensing interface which led to a major improvement in the detection of oligonucleotide hybridization using the electrocatalytic amplification of redox-labeled oligonucleotide-hybrids. The optimization was centered on the use of bifunctional bioconjugates to tailor the architecture and the performance of the electrocatalytic platform. We found that the use of SAv as an underlying layer affects the electroactivity of the interfacial architecture but promotes specific detection of the amplified electrochemical signal. Considering that the reduced amount of redox centers connected through the bioconjugate could impact the electrochemical signaling, we demonstrated that the electrocatalytic current can be easily amplified and/or tuned by simply increasing the concentration of the donors in solution. More importantly, further amplification of the electrocatalytic readout did not affect the performance of the platform. With an increase in the concentration of donors, the signal was amplified without interferences. In addition to the stability, the strong dependence of the detected signal on the surface density of the targets enabled us to use this interfacial architecture for probing oligonucleotide with a detection limit in the picomolar regime. This modular molecular architecture system provides a robust, sensitive, and versatile platform for detecting oligonucleotide hybridization.

ACKNOWLEDGMENT

O.A. acknowledges financial support from the Alexander von Humboldt Foundation and the Max Planck Society.

Received for review March 18, 2008. Accepted June 24, 2008.

AC800560T

(46) Li, D.; Yan, Y.; Wieckowska, A.; Willner, I. *Chem. Commun.* **2007**, 3544–3546.